# Demand-side Management of Air Conditioning Cooling Loads for Intra-hour Load Balancing

Yu Zhang, *Member*, *IEEE* and Ning Lu, *Senior Member*, *IEEE*

***Abstract* — This paper evaluates the performance of a centralized load controller designed to provide intra-hour load balancing services (LBSs) using air conditioning (a/c) units in their cooling modes. First, thermal models of a/c units and the control logic of the central controller are presented. The objective is to control the aggregated consumption of the thermostatically controlled appliances (TCAs) to follow a desired load profile for providing LBSs. The simulations are carried out in a MATLAB/Simulink environment. A total of 1000 a/c units in their cooling modes are modeled to provide a realistic ±1 MW load balancing signal for 24 hours for baseline settings. The impacts of lockout times, ambient temperatures, heat gains, and two-way communication delays on the demand-side management (DSM) performance are modeled. The cost of communication between the TCAs and the central controller, customer comfort, device life cycles, and control errors are used as metrics to evaluate the DSM performance. The results demonstrate that the DSM controller precisely controls the aggregated heating, ventilating, and air conditioning load shapes while maintaining load diversity. The controllable and the measurable load services that the controller provides can be used for many other demand response applications, such as peak shaving, load shifting, and arbitrage.**

**Index Terms— demand response, load management, direct load control, thermostatically controlled appliances, ancillary service, renewable integration, smart grid, optimal parameter selection.**

## I. Introduction

The ramp-rate and magnitude of load balancing services (LBSs), such as load following and regulation, will increase rapidly when the penetration of intermittent renewable energy resources on the power grid exceeds 10% [1]. Historically, a capacity margin of 20% has been considered sufficient to provide adequate generation security results at lower efficiencies [2]. To meet increased ramp rate requirements, faster regulating movements are required, which increases mechanical stress on generators, shortens generator lifetimes, and increases wear-and-tear costs [3]. Energy storage resources, such as batteries [3], flywheels [4], and demand-side management (DSM) [2], are flexible energy options that could provide the needed fast-response ancillary services. Of these options, DSM is the most underutilized for LBSs [5]. This is because the fast load balancing service should be available whenever needed; it should be fully controllable, observable, and measurable to become a product in the ancillary service market. In addition, loads must be aggregated to the megawatt level to be practical to bid into the ancillary service market under current market rules. Nevertheless, since May 2006, markets for regulation service from DSM programs have opened in Pennsylvania, New Jersey, the Maryland Interconnection, and the PJM Interconnection LLC, although because of the strict telemetry requirement, all the participants of these programs so far have been large industrial customers [5], [6].

Advanced metering infrastructure (AMI) is receiving the most attention with the emerging concept of smart grid to improve DSM, increase energy efficiency, and allow a self-healing electrical grid [7]. Approximately 39 million meters have been installed since 2010 [8]. Traditional interruptible demand at industrial plants is moving toward demand response programs that either allow an energy service provider to perform direct load control (DLC) or provide financial incentives for customer-responsive demand at homes and businesses [7]. Indirect load control with one-way communication is an open-loop control mechanism and may not be suitable to provide LBSs that have strict magnitude, duration, and ramp requirements under current electricity market settings. In DLC [9], the load is controlled directly by a utility or a system operator, making it possible to adjust the consumption precisely. Therefore, DLC has been selected in this study to demonstrate the applications of providing LBSs using TCAs. To gain consumer acceptance, the control implementation needs to be low-cost, profitable, and non-intrusive. Consumers must also be able to override the centralized control when they no longer want to participate.

The direct control of electric water heaters (EWHs) to adjust their power consumption to follow regulation signals has been investigated in [10]. Because no resource prioritization is made in the approach, the EWHs being switched on or off may not have been the optimal ones to be on or off. As a result, more than 10,000 EWHs were required to provide ±1 MW regulation services. To improve resource utilization, increase control efficiency, and maintain load diversity and customer comfort, a temperature priority list method proposed in [11], [12] is used to prioritize each space heating unit based on how close it is to being turned on or off.

In this paper, an equivalent thermal parameter (ETP) residential air conditioning model is used and a forecaster of the room temperatures is applied at the central controller to forecast TCA behavior on a 0.01 hour basis; the forecasts are corrected by measurements obtained from the AMI every several minutes (forecaster sample time) or so. Thus, the controller broadcasts control signals at the actual control interval, e.g., every time interval (0.6 minutes), but collects monitoring signals from

This work was conducted by Pacific Northwest National Laboratory, which is operated for the U.S. Department of Energy by Battelle under Contract DE-AC05-76RL01830. Dr. Y. Zhang and Dr. N. Lu is with the Energy Science and Technology Division, Pacific Northwest National Laboratory, Richland, WA, 99352, USA. Email addresses: Yu.Zhang@pnnl.gov; ninglu134@gmail.com .

each TCA at every forecaster sample time. Doing so significantly reduces the communication and computational burdens. The central controller controls the on and off status of each TCA load while maintaining its temperature within desired ranges.

This paper presents a second-order residential ETP air conditioning model, forecaster design, and setup for the baseline and control signal in Section II and introduces the control algorithm for providing ancillary services in Section III. The modeling results of the impacts of imperfect forecast, lock-off time, delay response, and outdoor temperature are presented in Section IV. The conclusions are summarized in SectionIV.C.

## II. Modeling Methodologies

A heating, ventilation, and air conditioning (HVAC) load is used to illustrate the control algorithm development. To model the electricity consumption of an HVAC unit, it is critical to model the unit's heat transfer process (as shown in Fig. 1), considering ambient temperature changes. This section introduces the thermal dynamic equations.

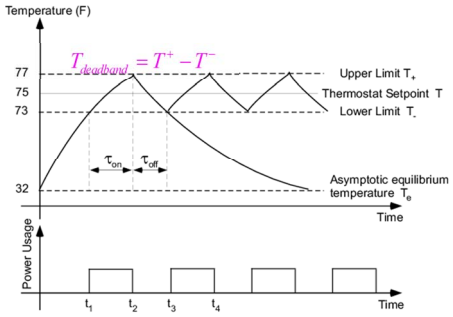


Fig. 1: Thermal behavior of an HVAC unit.

### A. Thermal Dynamic Models of an HVAC Unit

An ETP model [13] of a residential HVAC unit is shown in Fig. 2, in which parallel or nearly parallel heat flow paths and series thermal mass elements are grouped into a few parameters and portrayed as a simple direct current (DC) electric circuit [14].

A state space description of the ETP model is

$$\dot{x} = Ax + Bu \qquad (1)$$
$$y = Cx + Du$$

$$x = \begin{bmatrix} T_i \\ T_m \end{bmatrix} \qquad u = \begin{bmatrix} T_0 \\ Q_a \\ Q_m \end{bmatrix}$$

$$A = \begin{bmatrix} -\frac{U_a + H_m}{C_a} & \frac{H_m}{C_a} \\ \frac{H_m}{C_m} & -\frac{H_m}{C_m} \end{bmatrix} \qquad B = \begin{bmatrix} \frac{U_a}{C_a} & \frac{1}{C_a} & 0 \\ 0 & 0 & \frac{1}{C_a} \end{bmatrix}$$

$$C = \begin{bmatrix} 1 & 0 \end{bmatrix} \quad D = \begin{bmatrix} 0 & 0 & 0 \end{bmatrix}.$$

$C_a$ – air heat capacity (Btu/°F)
$C_m$ – mass heat capacity (Btu/°F)
$Q_a$ – the heat flux to the interior air mass (Btu/hr)
$Q_m$ – the heat flux to the interior solid mass (Btu/hr)
$U_a$ – the conductance between the inner and outer air mass (Btu/°F·hr)
$U_m$ – the conductance between the inner air mass and the inner solid mass (Btu/°F·hr)
$T_o$ – ambient temperature (°F or °C)
$T_i$ – air temperature inside the house (°F or °C)
$T_m$ – mass temperature inside the house (°F or °C)

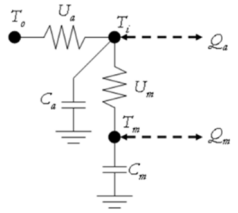


Fig. 2: ETP model of a residential HVAC unit.

The detailed model can be simplified by considering an equivalent model that matches the measured turn-on time, $t_{on}$, and turn-off time, $t_{off}$, under a range of ambient temperatures, $T_o$.

When the cooler is turned on, $Q_a$ will subtract or add $Q_{hvac}$, which is the air heat reduced or increased by the TCA; when it is turned off, $Q_{hvac}$=0.

### B. Forecaster Design

To mitigate the cost of bi-directional communication between TCAs and the central controller, a forecaster is designed. The full dynamic model produces satisfactory results and updates room temperatures for the forecasting process every 6–15 minutes to create a temperature priority list for a large number of HVAC units. Even if an imperfect forecaster is utilized, the central controller will read the user data every couple minutes and update it in the forecaster so that it will correct the room temperature accordingly.

In the forecaster of the central controller, we use linearized turn-on and turn-off curves to forecast the TCA temperature. The forecaster can calculate the temperature changes using (2) and (3).

When the cooler is turned off,

$$T_{room}^{t+1} = T_{room}^{t} + k_{up}\Delta t \,. \qquad (2)$$

When the cooler is turned on,

$$T_{room}^{t+1} = T_{room}^{t} - k_{down}\Delta t \,. \qquad (3)$$

$T_{\text{room}}$ – room temperature (°F)
$t$ – time
$\Delta t$ – time step
$k_{up}$ – ramp rate of indoor temperature increase
$k_{down}$ – ramp rate of indoor temperature decrease

During our simulation, each HVAC unit is modeled using the detailed model described by (1). The forecaster located in the central controller uses the simplified methods to estimate indoor temperature of each house. The linearized forecaster model is easy to derive based on measurement data.

In the rest of this paper, 1000 HVAC units (rated at 6 kW) in their cooling modes are modeled to illustrate the algorithm and the control mechanism. Consumer thermostat set point settings, $T_{\text{set}}$, are set at 75°F. $T_{\text{deadband}}$ is the temperature deadband. Set $T^+$ to be 75°F+0.5 $T_{\text{deadband}}$ and $T^-$ to be 75°F+0.5 $T_{\text{deadband}}$.

### C. Set Up the HVAC Baseline Output

An aggregated baseline output of the HVAC units, $P_{baseline}$, must be provided to grid operators so that deviations from the

baseline output can be measured as continuous regulation reserves (CRRs), e.g., regulation up and down services or load following up and down services.

To create a baseline load, all participating HVAC units are modeled in an uncontrolled mode using next-day outdoor temperature forecasts. The uncontrolled mode means that HVAC thermostats turn the HVAC units on and off. Then, the aggregated HVAC power output is averaged to an hourly load profile as the day-ahead $P_{baseline}$, as shown in Fig. 3. Note that the baseline load profiles vary with outdoor temperature, thermostat settings, and the number of controlled HVAC units. In general, more HVAC units and wider dead band settings provide greater load balancing capacity.

### D. Control Signals

Load following signals [1] are scaled to 1 minute and normalized to ±1 MW for a baseline load constructed by 1000 controlled HVAC units. The control signal, $P_c^{Reg}$, is calculated as

$$P_c^{Reg} = P_{Baseline} + P_{Reg} \,. \tag{4}$$

An example of the control signal for controlling the 1000 HVAC units for ±1 MW load following is shown in Fig. 3.

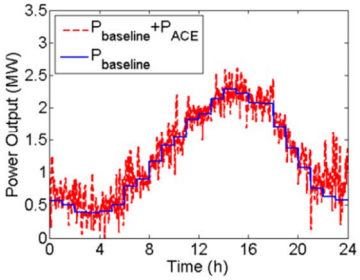

Fig. 3: Baseline loads and control signals.

## III. Control Algorithms

A flow chart of the DLC logic is provided in Fig. 4. The key steps are to group and prioritize resources based on forecaster results. Before the controller starts the dispatch algorithm, all of the controllable HVAC units are first divided into two groups based on their forecasted on/off status. As space cooling units are used in this paper for demonstration purposes, the units in the "on" group are prioritized in ascending order based on their room temperatures, i.e., if the room temperature is closer to the upper thermostat setting $T^-$, the unit is at the top of the queue to be turned off. The units in the "off" group are prioritized in descending order based on their room temperatures, i.e., if the room temperature is closer to the lower thermostat setting $T^+$, the unit is at the top of the queue to be turned on. The HVAC units that are "on" under DLC will switch off immediately when they receive an "off" signal from the central controller, and vice versa.

As shown in Fig. 5, if all HVAC units are grouped into five "on" states and five "off" states, the units in State 1, which are darkest in color in Fig. 5, will have the highest priority to be used. This is because if we turn off an "on" HVAC unit (e.g., a unit in State 1 in the "on" group), which is close to $T^-$(73°F), the unit will stay longer in the "off" queue compared with other "on" units. In the case of a unit in State 5 in the "on" group, if it is turned off, it will spend less time in the "off" queue since it was just turned on. This is an optimal way to use the "on" HVAC resources compared with sending an "off" command to a random HVAC unit in the "on" group.

If we turn on an "off" HVAC unit in State 1, which is close to $T^+$(77°F), it will stay longer in the "on" queue compared with other "off" units (e.g., a unit in State 5 in the "off" group). This is an optimal way to use the "off" HVAC resources compared with sending an "on" command to a random HVAC unit in the "off" group.

Another advantage of this control mechanism is that it has a minimal impact on load diversities. Assuming there is one HVAC unit in each state without a control signal, as shown in as Fig. 5, after an applied control signal that requires one unit to be turned on, one HVAC unit in State 1 should be turned on, as shown in Fig. 6. If we use the temperature priority list and control the on/off status of the HVAC unit directly, only one unit in State 1 from the "off" group moves to the "on" group. There is only one state with zero population and one state with an increased population among all 10 states.

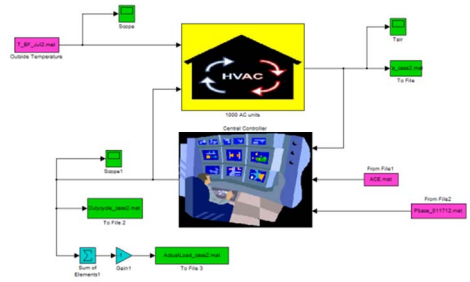

Fig. 4: Flow chart of HVAC control logic.

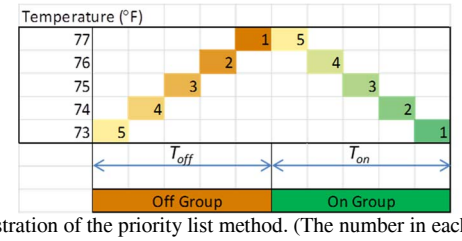

Fig. 5: Illustration of the priority list method. (The number in each block represents the state number.)

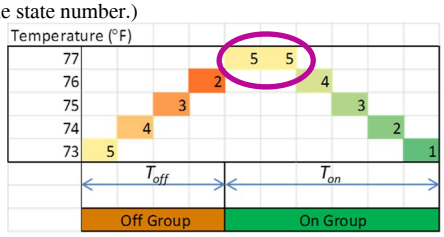

Fig. 6: Illustration on the state evolution using temperature priority list method.

The forecaster is used to estimate room temperatures of the HVAC units for the next time step, determine the on/off status of the HVAC units, and create two priority (turn-on and turn-off) lists for the two groups of HVAC units. The forecasts, $T_f^{HVAC}$, can be tuned and corrected based on actual measurement, $T_a^{HVAC}$, collected from HVAC units every 6–15 minutes (that could change). The forecaster can use a simplified HVAC thermal model as described in (2) and (3) in Section II.B. A forecast-and-update process, as shown in Fig. 7, will reduce the amount of data traffic from each controlled HVAC unit to the central controller.

## IV. Modeling Results

Our experiment is based on a GridLab-D two-order ordinary differential equation (ODE) residential HVAC model. House sizes vary from 1500 sqft to 4000 sqft under uniform distribution. Each air conditioning model has unique parameters. In our study, HVAC models are in cooling mode.

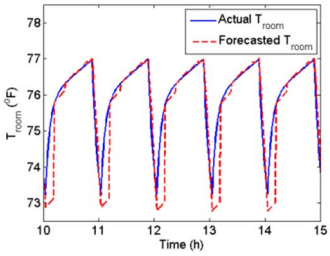


Fig. 7: Room temperature profiles of an HVAC unit in heating model (modeled by (2) and (3) and tuned by measurements).

In the base case, the central controller receives room temperature measurements at each time step with no communication delays in sending control commands or receiving monitoring data. In addition, the HVAC units respond to control commands immediately, with no turn on/off delays. This assumption is made to explore the full potential of the HVAC units to provide CRR services when the central controller has precise information and instantaneous control of each HVAC unit. Then, several factors that may limit the capability of the HVAC load for CRR services are simulated. First, the impact of the update-by-measurement process is modeled in the imperfect forecast case. When an HVAC unit is turned off, a lock-off time (see Fig. 8), $T_{\min}^{off}$, is set to lock the HVAC unit out of the "on" group to prevent the unit from stalling; this case is modeled in the lock-off time case. The influence of outdoor temperature on the quality of CRR services is studied in the case of outdoor temperature impact. Then, the turn-on delay (see Fig. 8), $T_{delay}^{on}$, and turn-off delay (see Fig. 8), $T_{delay}^{off}$, which are caused by communication and response delays, are modeled in the response delay case.

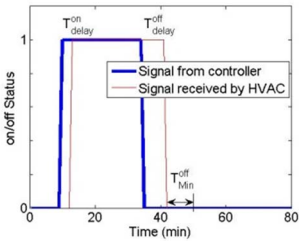


Fig. 8: Response delays and minimum turn-off time.

In this paper, the above points on the control performance are discussed.

### A. Base Case

Load following signals are scaled to 1 minute and normalized to ±1 MW for a baseline load constructed by 1000 controlled HVAC units, as shown in Fig. 3 in Section II.D. The following observations are made from simulation results:

- The HVAC load follows the control signals very well for a deadband of 4°F as shown in Subplot 1, Fig. 9.
- As shown in Subplot 2, Fig. 9, the indoor temperatures are kept within their high and low limits; the centralized-dispatch algorithm simply changes the cycle length of each HVAC unit to obtain an aggregated load profile that matches the control signal.
- Each HVAC unit is switched on/off approximately 8–22 times per day (see the blue line in Subplot 3, Fig. 9); to provide the 1 MW load following service, each HVAC unit will be switched on/off 1.5 times more often when deadbands are set at 4°F.

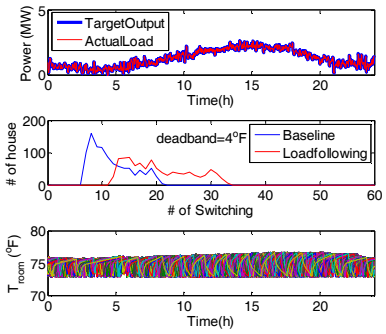


Fig. 9: Results for the base case.

### B. Imperfect Forecast Case

Two scenarios are simulated: $T_{\text{deadband}}$ = 4°F and $T_{\text{deadband}}$ = 3°F. The outdoor temperature in both scenarios is 80–99°F for a peak summer day. Simulation results are shown in Fig. 10 through Fig. 12, in which Subplot 1 shows target output load and actual load, Subplot 2 compares the switching time of baseline with that of each case, and Subplot 3 shows indoor temperatures. These figures demonstrate the following:

- The forecaster update algorithm is effective. Because the forecaster located at the control center is only an approximation of the real HVAC unit, it will have prediction errors. In some cases, the forecast error may be significant, as shown in Fig. 10.
- The simplified HVAC model, adjusted every 12 minutes by meter data representing the HVAC load, effectively provides load following service (Subplot 1, Fig. 11). If every 12 minutes the error can be corrected by measurements collected from the AMI network, the forecaster can predict the HVAC unit's state relatively well. The adverse impacts are that the HVAC unit will be switched on/off 2–5 more times per day (Subplot 2, Fig. 11), and a small portion of room temperatures may exceed 73°F by half a degree or so. This is because if the forecast is inaccurate, the HVAC unit may be turned on or off for a couple more minutes than are actually needed (Subplot 3, Fig. 11). This may inconvenience some consumers.
- When $T_{\text{deadband}}$ changes to 3°F in Fig. 12, compared to Fig. 11 when $T_{\text{deadband}}$ is 4°F, it shows that a larger deadband will give system a larger control capacity. From Fig. 12.(a) and Fig. 12.(b), the differences between target load and actual load decrease as forecaster sample time changes from 12 min to 6 min. When $T_{\text{deadband}}$ is set to 3°F and forecasters use a 12 min sample time, actual load cannot track target output at peak hour in Fig. 12.(a). On a peak summer day, the maximum ambient temperature in this study is approximately 99°F and the

average is approximately 87°F. When the temperature rises to the peak value, many HVAC units are saturated, and thus the output power cannot easily follow the control signal, especially if the forecasters are not perfect and sample time is too long. However, when the forecaster sample data time decreases to 6 min in Fig. 12.(b), the forecast values of indoor temperatures are more accurate, and the output power could follow the control signal well. This study shows the system output power limitation based on forecaster sample data time.

- A possible solution to room temperature violations is to narrow $T_{\text{deadband}}$, as shown in Fig. 12. The results show trade-offs among consumer comfort and appliance lifetimes and forecaster sample time because if the temperature band is set to be narrower, the HVAC unit will be switched on/off more often, as shown in Subplot 2, Fig. 12.(b), and the forecaster sample time has to be made smaller to follow control signal at peak hour.
- Note that if the $T_{\text{deadband}}$ is changed from 4°F to 3°F, the baseline load will change as well. A narrower $T_{\text{deadband}}$ requires more frequent HVAC unit cycles.

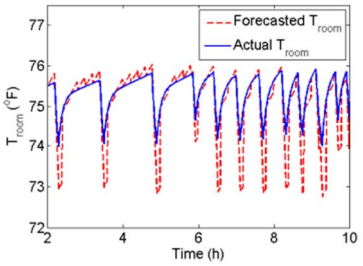


Fig. 10: Forecast correction process of an HVAC unit.

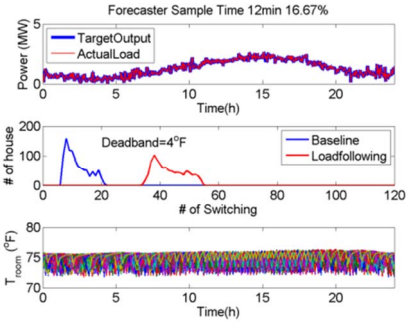


Fig. 11: Results for the imperfect forecast case: 12 min forecaster sample time ($T_{deadband}$ = 4 °F).

## C. Lock-off Time

Lock-off time is an HVAC unit's minimum off time, which means that after a unit is turned off, it need this amount time at least before it can be turned on. We run two scenarios: lock-off time is equal 3 min and 8 min for each HVAC unit when $T_{deadband}$ is 4 °F, shown in Fig. 13. Because the priority list method sorts the HVAC units by room temperature, the controller will first turn off units that are close to $T^-$, and turn on units that are close to $T^+$. Subplot 1, Fig. 13 show that off state duration of a unit; Subplot 2, Fig. 13 shows the comparison of original switch on-off signal and that after applied lock-off time; Subplot 3, Fig. 13 shows the total target and actual power of all the units. In Subplot 2, Fig. 13, "1" means on state and "0" means off state. From the results, we conclude that if the lock-off time of the HVAC unit is longer than 8 minutes, the control performance will be degraded significantly.

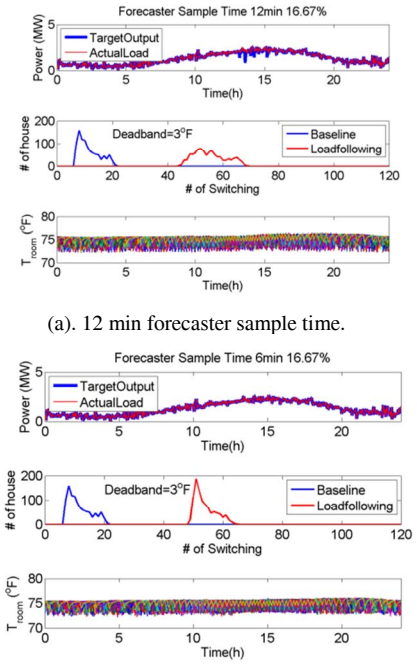


(a). 12 min forecaster sample time.

(b). 6 min forecaster sample time.

Fig. 12: Results for the imperfect forecast case: (a). 12 min forecaster sample time; (b). 6 min forecaster sample time ($T_{deadband}$ = 3 °F).

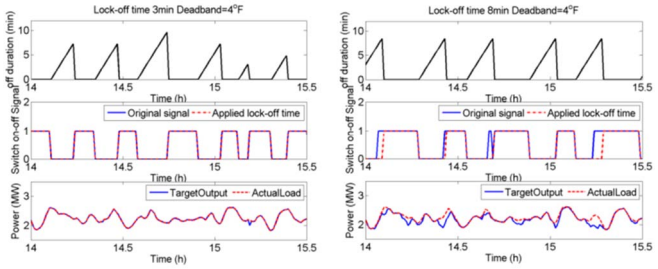


(a). 3 min lock-off time. (b). 8 min lock-off time.

Fig. 13: Results for different lock-off time cases: (a). 3 min lock-off time; (b). 8 min lock-off time ($T_{deadband}$ = 4 °F).

## D. Outdoor Temperature Impact

When an HVAC unit works in the cooling mode, the results will be driven by outdoor temperature characteristics. As shown in Fig. 14 (hour 2–hour 13), if outdoor temperatures are below or very close to the cooling thresholds, the HVAC units may not be turned on or will only be turned on briefly. Their capabilities to adjust consumption are very limited.

## E. Response Delay

This case is designed to test how much tolerance the control mechanism has for response delays from resources that are not only geographically distant from each other but also different in design. The delay may be caused by communication issues or other factors, the nature of which are not discussed in this paper. Communication delay usually is a value in milliseconds to seconds. We use a 0.6 min delay in these cases, which is adequate for delay tests.

To model the impact of the response delay on the load following capability of the aggregated HVAC load, three scenarios are modeled:

- 99% chance to react immediately and 1% chance to have a 0.6 min random response delay
- 95% chance to react immediately and 5% chance to have a 0.6 min random response delay
- 50% chance to react immediately and 50% chance to have a 0.6 min random response delay

Percent errors of the cases with three different delay probabilities are shown in Fig. 15. The medians of 1% and 5% change delay cases are close to zero. The distance of the two "whiskers" is wider in the 5% case compared with the 1% case. The percent error of the 5% change delay case is higher than the 1% case. The mean of the 50% change delay case is approximately 75% below zero, which is highest among the three cases. The bias in percent error shows that when HVAC units fail to follow the control commands, the actual energy consumption falls below the target consumptions, resulting in large negative percentage errors. It demonstrates that the 2-way communication networks need to be reliable for the HVAC units to provide reliable services. In this case, the communication delays should not influence more than 5% HVAC units.

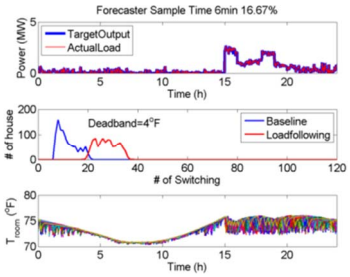


Fig. 14: Total power consuming, switching times, and room temperatures at an average 78°F outdoor temperature, 6 minutes forecaster sample time and no solar and internal heat gains.

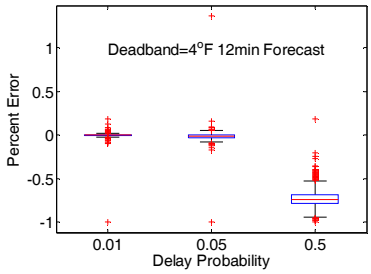


Fig. 15: Results for the response delays.

## V. Conclusions

This paper proposed a centralized controller for HVAC in a cooling model, presented the design considerations, and studied imperfect forecast, lock-off time, delay response, and outdoor temperature impact. First, two-order dynamic ETP house TCA models and a forecaster were designed in cooling mode, which is different from the simplified model in heating mode of our previous work. Then, the baseline aggregated HVAC power output was estimated from the modeled average load profile based on outdoor temperature forecast. Next, the control method of HVAC units for intra-hour load balancing was proposed. Additionally, operation of HVAC units was simulated in the MATLAB/Simulink platform. Finally, we studied the influence of several factors on the performance and standard of evaluation and parameter selection.

In this paper, we focused on evaluation of the performance of the HVAC cooling load for providing CRR services. The impacts of lock-off time, ambient temperature, the two-way communication delay on the performance were studied. The greater the lock-off time of the TCA units, the larger the change of delay, which can downgrade system performance. The temperature profile, which has a strong influence on the system performance, is also a significant factor on services.

The results indicated that approximately 1000 HVAC units (rated at 6 kW with 4°F dead band) can provide 24 hours of intra-hour continuous balancing services (1-MW bi-directional signals) by the proposed control scheme. With a smart grid in place, load service providers can extend the control to TCAs and collect additional revenue from the ancillary service market to recover the cost invested in the two-way communication and control network. Consumers can also receive additional revenue by offering their appliances for load balancing services and help integrate more renewable resources into the power grid without compromising their comfort levels.

## References


[1] Y.V. Makarov, C. Loutan, J. Ma, and P. de Mello, "Operational impacts of wind generation in California power system," *IEEE Trans. on Power Systems,* vol. 24, no. 2, pp. 1039-1050, 2009.

[2] G. Strbac, "Demand Side Management: Benefits and Challenges," *Energy Policy*, vol. 36, no. 12, pp.4419-4426, 2008.

[3] N. Lu, M.R. Weimar, Y.V. Makarov, J. Ma, and V.V. Viswanathan, "The Wide-Area Energy Storage and Management System - Battery Storage Evaluation," Pacific Northwest National Laboratory, Richland, WA, Tech Rep. PNNL-18679, 2009.

[4] N. Lu, M.R. Weimar, Y.V. Makarov, F.J. Rudolph, S.N. Murthy, J. Arseneaux, and C. Loutan, "An Evaluation of the Flywheel Potential for Providing Regulation Service in California," *Proc. of the 2010 IEEE PES General Meeting*, Minneapolis, MN, U.S., July 2010.

[5] G. Heffner, C. Goldman, B. Kirby, M. Kintner-Meyer, "Loads Providing Ancillary Services: Review of International Experience," Lawrence Berkeley National Laboratory, Berkeley, CA, Tech. Rep. LBNL-62701, ORNL/TM-2007/060, PNNL-16618, 2007.

[6] M. Andreolas, "Mega Load Management System Pays Dividends," *Transmission & Distribution World*, Feb. 2004, pp. 33-37.

[7] U.S. Department of Energy, "Smart Grid System Report," 2009

[8] SmartGrid, Advanced Metering Infrastructure and Customer Systems. [Online]. Available: http://www.smartgrid.gov/recovery_act/deployment_status/ami_and_customer_systems

[9] N. Lu and D.P. Chassin, "A State Queueing Model of Thermostatically Controlled Appliances," *IEEE Trans. on Power Systems*, vol. 19, pp. 1666-1673, 2004.

[10] J. Kondoh, N. Lu, and D.J. Hammerstrom, "An Evaluation of the Water Heater Load Potential for Providing Regulation Service," *IEEE Trans. on Power Systems*, issue 99, 2011.

[11] N. Lu, "An Evaluation of the HVAC Load Potential for Providing Load Balancing Service," *IEEE Trans. on Smart Grid*, to be published.

[12] N. Lu, "Design Considerations of a Centralized Load Controller Using Thermostatically Controlled Appliances for Continuous Regulation Reserves," *IEEE Trans. on Smart Grid*, submitted for publication.

[13] S. Katipamula and N. Lu, "Evaluation of Residential HVAC Control Strategies for Demand Response Programs," *ASHRAE Transactions*, vol. 1, no. 12, pp. 1-12, 2006 (PNNL-SA-45954, Pacific Northwest National Laboratory, Richland, WA).

[14] GridLab-D, Residential Module Guide, [Online]. Available: http://sourceforge.net/apps/mediawiki/gridlabd/index.php?title=Residential_Module_Guide